International Journal of Engineering Inventions
e-ISSN: 2278-7461, p-ISSN: 2319-6491
Volume 13, Issue 6 [June. 2024] PP: 213-219

An Experimental Study of Swarf in the Sawing of Granite with Diamond Wire

Le Nhu Trang[1*]
**Corresponding Author*

Abstract*—*A diamond wire-sawing process was developed to slice granite in both quarries and block processing plants. Swarf was collected from different areas along the sawing arc during the wire sawing of three granites. Furthermore, the particle size distribution and the morphologies of the swarf were investigated systematically, along with the swarf formation mechanism in sawing. Swarf formation in the granite was dominated by transgranular fractures based on the morphology of a sawn granite chip and the analysis of sawn chip size. A long cutting arc increased the movements among the swarf, tool, and workpiece, thereby inducing a secondary fracture in the sawn chip.

***Keywords*—** *Diamond wire, sawing, granite, swarf.*

Date of Submission: 14-06-2024 Date of acceptance: 27-06-2024

I. INTRODUCTION

Diamond wire cutting technology was first used in the quarries from which soft stone is extracted, including marble. Hence, diamond wire saws are most widely used in both quarries and block processing plants to cut marble. Diamond wire saws were first used to extract hard stone, such as granite, gneiss, and diorites, from quarries in the 1980s. Since then, diamond wire technology has become the tool of choice in hard-rock quarrying as a result of the development of diamond-wire cutting machines and of diamond wire itself since 2000. This technology has significantly improve the production rate and overall efficiency of cutting [1, 2].
Unlike circular sawing and wheel grinding, diamond wire sawing displays the following common machining characteristics.

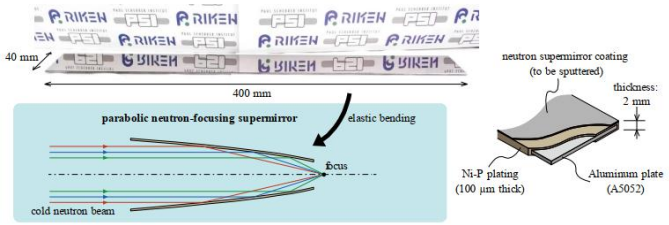

Fig. 1: Thin metal substrate with a Ni-P plating for the neutron supermirror deposition and its usage as bent parabolic neutron-focusing mirrors.

Long cutting arc. The length of the contact of the diamond wire with the workpiece is several meters in block processing plants and dozens of meters in quarry wire sawing. These lengths are hundreds or thousands of times longer than that of the traditional circular sawing arc, as shown in Fig. 1.
Flexible cutting mode. Diamond wire is more flexible than circular sawing and grinding. Thus, it can be bent during cutting because of the elasticity of the twist steel, as illustrated in Fig. 1. The degree of bending is closely related to cutting feed rate. Diamond beads retreat when the cutting force is too strong as a result of this flexible cutting mode, which prevents a violent collision between the diamond grain and the workpiece.
Much research has focused on the machinability of natural stones and on developing efficient tools for granite sawing to improve sawing performance and reduce cost. Butler–Smith et al. evaluated the performance of individual beads using an apparatus that was specially designed for bead wear and friction testing [3]. Özçelik et al. optically investigated the effects of the structure ofdiamond beads and rock types on the wear of diamond beads during cutting [4]. These studies provided fundamental knowledge regarding bead wear in sawing. Jain et al. also numerically predicted the cutting performance of diamond wire saws in marble quarrying using a neural network approach [5]. The effects of machining parameters have also been investigated in the diamond wire sawing of rock, including wire speed, feed rate, cutting length, and segment diameter [6, 7]. Although the aforementioned studies provide important insight regarding machining processes and the tool wear mechanism during wire sawing, the prevailing mechanisms of swarf formation have not been clarified thoroughly and

quantified. Moreover, the full potential of this process is limited by the lack of a fundamental and systematic understanding of the material removal mechanism.

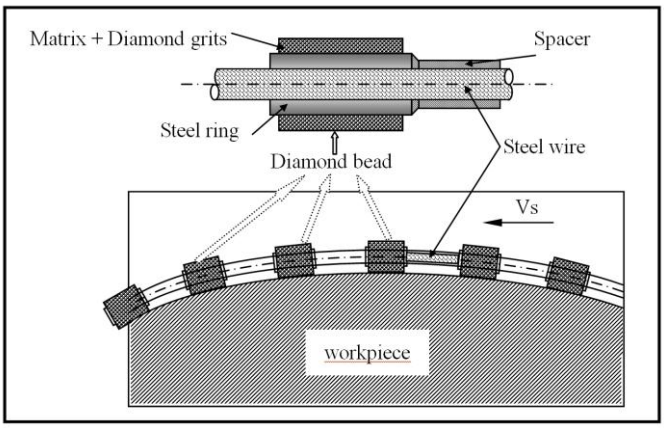

Fig. 1 Illustration of the diamond wire sawing

The current paper reports our recent studies on the characteristics and formation mechanism of swarf in granite-wire sawing. The sawing tests are performed with our specially developed apparatus, which utilizes a steel wire impregnated with diamond beads. The sawn swarfs are collected from different areas along the sawing arc during the wire sawing of three granites. Furthermore, the particle size distribution (PSD) and the morphologies of the sawn swarfs are investigated systematically. Finally, the swarf formation mechanism is discussed.

II. EXPERIMENTAL CONDITIONS

The wire-sawing experiments were conducted with a developed apparatus at a spindle power of 5.5 kW, as presented in Fig. 2. The diamond wire used in the experiments was specially designed for granite and is 5.5 m long. Moreover, its maximum wire speed is 45 m/s. The spacing of the guide wheel is 0.8 m. Wire tension was maintained at 1.5 kN in all of the experiments to ensure that the wire remained almost straight (without apparent bowing) during sawing. Thirty-seven abrasive beads were fixed to the wire per meter length. The cylindrical diamond bead had a diameter of 10.5 mm and a length of 7.6 mm. It contained diamond abrasives with mesh sizes of 40/50 and 30/40 (in US standard) at 23.25% and 6.75% volume percentage concentrations, respectively. The diamond beads were dressed by gently rubbing a refractory brick that was installed on the machine for 0.13 m2 until the diamond grains were fully exposed. The wire speed and the feed rate for dressing remained constant at 22 m/s and 8 mm/min, respectively.

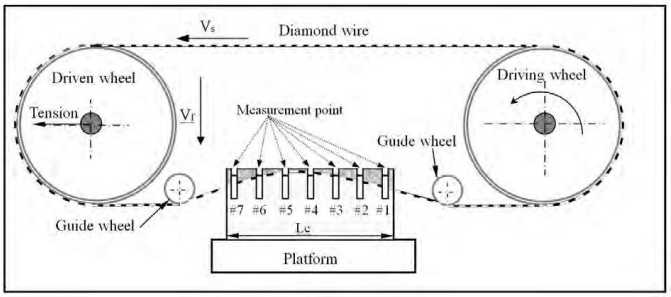

Fig. 2 Illustration of the measurement setup

Three kinds of natural granites were selected for the experiments at various grain sizes. Thin sections were prepared from each granite sample. Petrographic studies were conducted using a Leitz Wetzlar polarizing microscope, including the determination of the modal composition and the grain sizes of the studied granites. These examinations are depicted in Fig. 3. The sample granites mainly consisted of quartz, plagioclase, K-feldspar, biotite, and pyroxene. Quartz, feldspar, and biotite were considered the main minerals in granite composition. Table 1 summarizes their compositions and mechanical properties and lists the ranges of the mineral grain sizes of the three investigated granites. The test specimens were rectangular, 600 mm long, 200 mm wide, and 200 mm thick. The wire speed and the feed rate remained constant at 25 m/s and 8 mm/min, respectively, in the sawing experiments. Water coolant was applied at a constant flow rate of 6 L/min.

(a)Physical map of G657 (b)Physical map of G603 (c)Physical map of G654

Fig. 3 Physical map of granite in experiment

Swarf collection

To collect the swarf in the sawing zone, the granite chips sawn in the steady sawing state were guided into sample containers through a slope groove that was cut out previously when the diamond wire was completely sawn into the granite as in Fig. 4. This slope groove was 10 mm wide. Slope grooves were cut in different areas along the sawing zone according to the experiment process during sawing, such that all sawn chips along the long sawing arc could be obtained. To limit the influence of slope grooves on the collected chips, the chips were transferred from the final location of the workpiece to its starting point. First, groove #1 was cut near the final workpiece location, and a chip was collected from this groove in the long sawing zone. Groove #2 was then cut and a chip obtained from this groove, and so on. The first groove was 25 mm away from the starting location. The distance between two grooves was fixed at 100 mm. To stabilize the state of the cutting process, the total sawing depth was 15 mm in each sawing experiment.

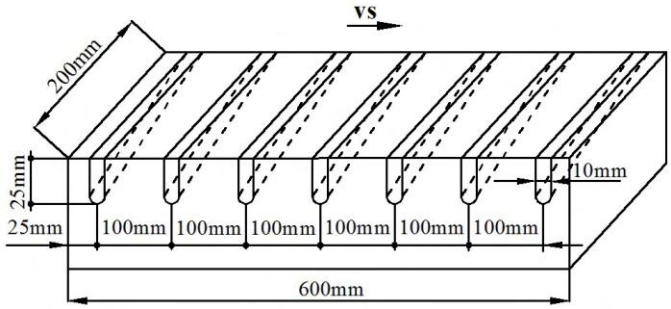

Fig. 4 Illustration of the sampling grooves distribution

Observation of swarf morphology

The sawn chip was sieved into various sizes through a series of mesh screens. The micro-morphologies of the chips were examined using a scanning electron microscope (SEM PHENOM). The chips were cleaned with acetone prior to examination. The mineral components of the swarf were also identified using the optical microscope system Hirox-KH8700.

PSD analysis

Chip PSD was measured with a laser diffraction particle size analyzer LS13-320. The collected chips were kept in a sampling container for 24 h until the sedimentation process was completed. 0.25 g of the deposited chip was diluted 2 g/L with distilled water. The refractive index of this water was 1.33; however, the accurate refractive index of granite was difficult to determine given its complex mineral composition. Quartz and plagioclase are the minerals that mainly comprise the three investigated granites, as shown in Table 1. Therefore, the refractive index of granite was set at 1.6 in this experiment because the refractive indices of quartz and plagioclase were 1.644 and 1.525, respectively. Sodium hexametaphosphate was used as a dispersant to scatter particles uniformly in the solution. The particle solution was subject to ultrasonic at 100 W power for 120 s during chip size analysis. The statistical duration of particle size analysis was 90 s.

III. EXPERIMENT RESULTS

3.1 PSD of the granite swarf

Figure 5 depicts the PSDs of three granites measured at location #7. Most chips measured approximately 10 μm to 200 μm. However, granite chips in the experiment were occasionally large at 300 μm to 600 μm, as indicated in Fig. 5(b).

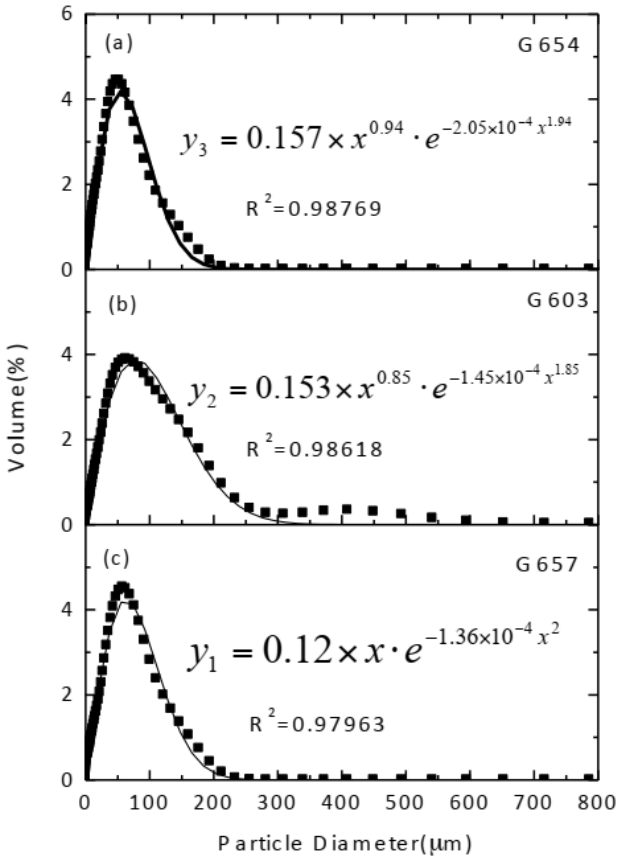

Fig. 5 Fitting result PSD of granite swarf with the lognormal distribution (measurement location #7)

The PSD is unimodal, as displayed in Fig. 5. Thus, it should be described by a mathematical distribution function to analyze the granite swarf quantitatively. The Weibull distribution effectively represents PSDs generated by grinding, milling, and crushing [8, 9]. It is still widely used to define PSDs in comminution. Therefore, the Weibull distribution was used to evaluate the sawn chips quantitatively after preliminary analysis. It accorded well with the PSD of the sawn chip indicated in Fig. 5.

The probability density function of a Weibull random variable is written as

$$f(x) = \left\{ \begin{matrix} 0, x < 0 \\ \frac{k}{\lambda} \cdot \left(\frac{x}{\lambda} \right)^{k-1} \end{matrix} \right\} . e^{-(x/\lambda)^k}, x \geq 0 \quad (1)$$

where $k > 0$ is the shape parameter and $\lambda > 0$ is the scale parameter of the distribution. The mean (E) of a random Weibull variable can be expressed as

$$E(x) = \lambda . \Gamma \left(1 + \frac{1}{k} \right) \quad (2)$$

where Γ is the gamma function.

The probability density function is fitted for each experimental result and presented in Fig. 5. The mean value of the sawn chips was calculated using Eq. 2. Figure 6 plots the mean size of the chips broken in different areas of the three granites, which ranged from approximately 40 μm to 80 μm. The mean value of the G603 chips, which were the largest of the three granites, varied between 68 and 77 μm. The mean value of the G657 chips ranged only from 45 μm to 65 μm, whereas that of the G654 chips was the lowest at only roughly 40 μm to 54 μm. The mean sizes of the sawn chips varied in the three granites; nonetheless, the sizes of the broken chips decreased slightly along the sawing zone in all of the experimental granites as depicted in Fig. 6.

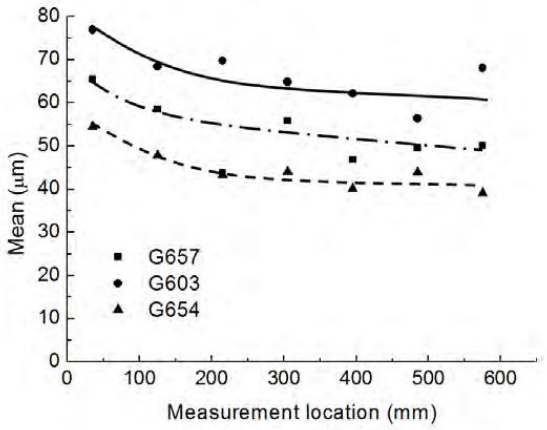

Fig. 6 PSD for three granites at different measurement locations

3.2 Morphology examinations

Figure 7 shows the typical optical micrographs of the swarfs with different PSDs. The colors of the sawn chips varied significantly in terms of their primary colors, which are black, white, brown, and clear. Multicolored granite chips could not be identified in all three examined granites with the exception of large chips, as indicated in Fig. 7a. The different colors indicate various mineral compositions and suggest that the swarf produced by wire sawing is composed of broken pieces of the minerals that constitute the granite. All minerals (quartz, feldspar, and mica) are represented over the entire range, from very fine to coarse particles. The three major minerals are magnified in Fig. 8.

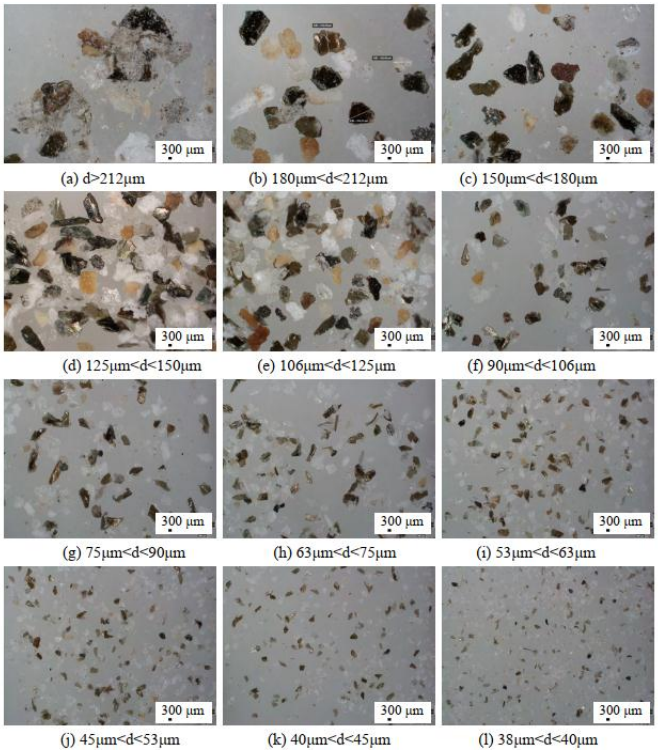

Fig. 7 Morphology of G657 swarf with different PSDs

Figure 9 exhibits the morphology of a chip with different mineral compositions as observed through SEM. Unlike the long, thin, and extruded filament-grinding chips of low-melting and soft ductile materials (mid steel) [10], granite generates blocky fracture particles. Figure 9(a) displays the conchoidal fracture feature, which is the typical fracture morphology in quartz. Mineral cleavage is incomplete in unfractured quartz as a result of external forces originating from a certain direction. Fractures or ruptures shape the quartz into smooth oval surfaces with a concentric pattern and similar hells. Figure 9(b) presents the feature of cleavage terrace on feldspar. Feldspar has either a triclinic or a monoclinic crystal system and two or three cleavage surfaces. Figure

9(c) shows the biotite, which is typical mica. This mica is monoclinic and has near-perfect basal cleavage as its most prominent characteristic. Its cleavage surface and fracture profile are indicated in Fig. 9(c) as well.

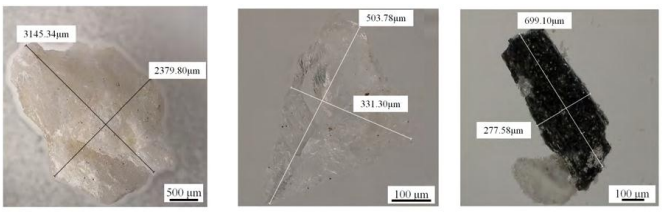

(a) Feldspar (b) Quartz (c) Biotite

Fig. 8 Magnification morphology of major swarfs

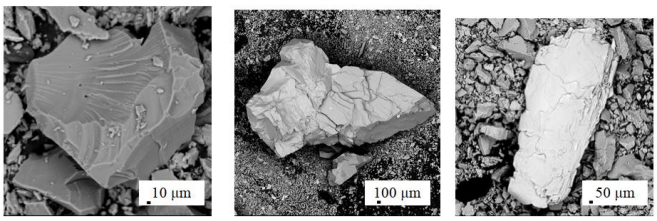

(a) Quartz (b) Feldspar (c) Biotite

Fig. 9 SEM micrographs of swarf with different mineral compositions

IV. DISCUSSION

This experiment obtained some large stone fragments that measure approximately 400 μm during wire sawing. This fragment size is similar to that of the grains of the mineral that comprise granite. The morphology of these large fragments is illustrated in Fig. 7(a), which are induced by the agglomeration of chip powder. This finding indicates that the sizes of sawn chips are much smaller than those of the mineral grains that constitute the stone. The stone is broken into particles during wire sawing under the action of the diamond grain. In previous studies, the features of granite fracture are dominated by the transgranular–intergranular fracture [11]. This fracture type is described by the means of the increments in distances within the mineral grains and along the grain boundaries. The chip with an intergranular fracture is similar in size to the original size of the mineral grain. This chip is larger than that with a transgranular fracture. In this experiment, the sawn chips are much smaller in size than the grains of the individual minerals that comprise this granite. This result suggests that the intergranular fracture is dominant in granite-wire sawing and that the binding forces among individual minerals must be greater than those within the minerals. Therefore, these minerals are never dislodged from their matrix as whole grains; rather, they are broken into fragments during wire sawing. This result is consistent with that of studies on the circular sawing of stone [12].

The sawn chips range from approximately 10 μm to 200 μm during wire sawing. These values are much higher than those obtained during the circular sawing [12, 13] and wheel grinding of stone [10]. However, the morphology examination results indicate that rock particles composed of several minerals cannot be identified, which is consistent with previous findings related to the circular sawing of stone [12, 13]. This chip morphology also suggests that chip formation is constant across different machining methods. The fracture particles of wire sawing are larger than those for circular sawing and grinding potentially because of the flexible cutting mode and the limited concentration of stress during wire sawing.

The mean size of the sawn chips varies across the three studied granites as in Fig. 6 despite their similar PSDs. In this experiment, G657 originally boasts the largest grain among the three granites; whereas G603 reported the largest mean chip size. The original grain size of G654 is the smallest among the three granites, as is the size of its sawn chips. This finding indicates that the original sizes of mineral grains are a factor that affects the size of a sawn chip. Moreover, mineral composition and flaw density influence chip formation significantly. Cleavage planes were observed in the SEM morphologies of the major mineral compositions, as indicated in Fig. 9. They facilitate the dislodgement of mineral fragments and are ideal initiation points for cutting. Minerals are typically broken into fragments before intact dislodging along the grain boundaries [12]. The highly incomplete cleavage in quartz broke the mineral into chips that were smaller than those of other minerals, although it corresponds to the hardness mineral in all mineral compositions. Therefore, the increased volume percentage of quartz may suggest that the mean chip size of G657 is smaller than that of G603.

The broken chips must be accommodated over the length of the cutting arc prior to release. The cutting arc in wire sawing is longer than that of circular sawing and grinding and can enhance the movements among the swarf, tools, and the workpiece. Reference [14] points out that diamond wear is mainly caused by grain

fractures and friction-induced wear. Moreover, the coolant and the swarf (chips) are combined to produce abrasive slurry that erodes the segment matrix. This erosion initiates a secondary fracture in the chip in combination with the friction with diamond grain, especially given the increased cutting arc. Thus, chip size decreases along the sawing zone (Fig. 6).

The movements among the swarf, tools, and workpiece are influenced by the following three items: workpiece chemistry and scratch resistance, the mean thickness of undeformed chips, and chip accommodation space [10]. The mean thickness of undeformed chips should be replaced with mean chip size in granite cutting because of the brittle removal method. Small particles are easier to accommodate than large particles at the same volume, and large chips may induce chip storage problems in wire sawing. The wear of the diamond tool in circular sawing is less than that observed during wire sawing because fine particles are easily accommodated in the space between the bond and work surfaces over the wheel-work contact arc.

V. CONCLUSION

Most chips range from approximately 10 μm to 200 μm during wire sawing. This range is smaller than those of the mineral grains that comprise the granite. A morphology examination of the sawn swarf indicates that granite chips composed of several minerals are difficult to identify. Moreover, wire sawing is dominated by an intergranular fracture. In addition, the PSD of the sawn chip conforms to the Weibull distribution. Mean swarf size decreased slightly along the sawing zone in all of the experimental granites and varied significantly with the changes in the granites. Finally, the sawn chip initiated a secondary fracture in the long cutting arc.

Acknowledgements

Hui Huang, ZRY, and XPX would like to acknowledge the financial support from the National Key Technology Support Program (2012BAF13B00), the National Natural Science Foundation of China (51175192, 51235004).

REFERENCES

NOTE: Do not use “et al.”

Format for books:

[1] D.N. Wright, J.A. Engels, The environmental and cost benefits of using diamond wire for quarrying and processing of natural stone, Industrial Diamond Review, (2003) 16-24.

[2] S. Kremshofer, H. Seebacher, Developments in diamond wire cutting for granite quarries, 1st International Conference on Stone and Concrete Machining, Hannover, Germany, 2011, pp. 33-38.

[3] P.W. Butler-Smith, J. Gryzagoridis, P.R. Davis, A single bead test for assessing diamond wire performance, Industrial Diamond Review, (1999) 93-101.

[4] Y. Özçelik, F. Bayram, Optical investigations of bead wear in diamond wire cutting, Industrial Diamond Review, (2004) 60-65.

[5] S.C. Jain, S.S. Rathore, Prediction of cutting performance of diamond wire saw machine in quarrying of marble: a neural network approach, Rock Mechanics and Rock Engineering, 44 (2011) 367-371.

[6] A.S. Robleda, J.A.V. Vilán, M.L. Lago, J.T. Castro, The rock processing sector: part i: cutting technology tools, a new diamond segment band saw part ii: study of cutting forces, Dyna, 77 (2010) 77-87.

[7] H. Huang, G. Huang, X.P. Xu, H. Huang, An experimental study of machining characteristics and tool wear in the diamond wire sawing of granite, Proceedings of the Institution of Mechanical Engineers, Part B: Journal of Engineering Manufacture, 227 (2013) 943-953.

[8] Y. Matsuo, T. Ogasawara, S. Kimura, Statistical analysis of the effect of surface grinding on the strength of alumina using Weibull's multi-modal function, Journal of Materials Science, 22 (1987) 1482-1488.

[9] C.Spero, D.J. Hargreaves, R.K. Kirkcaldie, H.J. Flitt, Review of test methods for abrasive wear in ore grinding, Wear, 146 (1991) 389-408.

[10] D.M. Pai, E. Ratterman, M.C. Shaw, Grinding swarf, Wear, 131 (1989) 329-339.

[11] R.J. Willard, J.R. McWilliams, Effect of loading rate on transgranular-intergranular fracture in charcoal gray granite, International Journal of Rock Mechanics and Mining Sciences & Geomechanics Abstracts, 6 (1969) 415-421.

[12] P. Hausberger, Stone machinability, Industrial Diamond Review, (1990) 258-261.

[13] N.G. Yilmaz, R.M. Goktan, Y. Kibici, An investigation of the petrographic and physico-mechanical properties of true granites influencing diamond tool wear performance, and development of a new wear index, Wear, 271 (2011) 960-969.

[14] X.P. Xu, Y. Li, The effects of swarf in the diamond sawing of granite, Key Engineering Materials, 250 (2003) 187-193.